

Numerical simulation of the $\mathcal{N} = (2, 2)$ Landau-Ginzburg model

Syo Kamata

*Graduate School of Science, Rikkyo University, 3-34-1 Nishi-Ikebukuro, Toshima-ku,
Tokyo 171-8501, Japan*

Hiroshi Suzuki

*Theoretical Research Division, RIKEN Nishina Center, Wako 2-1, Saitama 351-0198,
Japan*

Abstract

The two-dimensional $\mathcal{N} = (2, 2)$ Wess-Zumino (WZ) model with a cubic superpotential is numerically studied with a momentum-cutoff regularization that preserves supersymmetry. A numerical algorithm based on the Nicolai map is employed and the resulting configurations have no autocorrelation. This system is believed to flow to an $\mathcal{N} = (2, 2)$ superconformal field theory (SCFT) in the infrared (IR) that consists of a pair of $\mathcal{N} = 2$ minimal A_2 models. From a finite-size scaling analysis of the susceptibility of the scalar field in the WZ model, we determine $1 - h - \bar{h} = 0.616(25)(13)$ for the conformal dimensions h and \bar{h} , while $1 - h - \bar{h} = 0.666 \dots$ for the pair of A_2 models. We also measure the central charge in the IR region from a correlation function between conserved supercurrents and obtain $c = 1.09(14)(31)$ ($c = 1$ for the A_2 model). These results are consistent with the conjectured emergence of A_2 models, and at the same time demonstrate that numerical studies can be complementary to analytical investigations for this two-dimensional supersymmetric field theory.

Keywords: Supersymmetry, non-perturbative study, Landau-Ginzburg model, Nicolai map

Email addresses: skamata@rikkyo.ac.jp (Syo Kamata), hsuzuki@riken.jp (Hiroshi Suzuki)

1. Introduction

It is believed that the infrared (IR) limit of the two-dimensional $\mathcal{N} = (2, 2)$ Wess-Zumino model¹ (2D $\mathcal{N} = (2, 2)$ WZ model) with a quasi-homogeneous superpotential² is a non-trivial $\mathcal{N} = (2, 2)$ superconformal field theory (SCFT) [2, 3, 4, 5, 6, 7, 8, 9, 10]. See §19.4 of Ref. [11] and §14.4 of Ref. [12] for reviews. This Landau-Ginzburg (LG) description [13] of $\mathcal{N} = (2, 2)$ SCFT is a remarkable non-perturbative phenomenon in field theory and physically, for example, provides a basis for application of the gauged linear sigma model [14] to the Calabi-Yau compactification. Although the emergence of SCFT has been tested in various ways, it is very difficult to confirm this phenomenon directly in correlation functions, because the 2D WZ model is strongly coupled in low energies. Application of conventional numerical techniques (such as the lattice) would not be straightforward either, because supersymmetry (SUSY) must be essential in the above non-perturbative dynamics.

In a recent interesting paper [15], Kawai and Kikukawa revisited this problem and they computed non-perturbatively some correlation functions in the 2D WZ model by employing a lattice formulation of Ref. [16]. They considered the 2D $\mathcal{N} = (2, 2)$ WZ model with a massless cubic superpotential

$$W(\Phi) = \frac{\lambda}{3}\Phi^3, \quad (1.1)$$

which, according to the conjectured correspondence, should provide a LG description of a pair of the A_2 minimal models, where one is left-moving and the other is right-moving. In the IR limit, the scalar field in the WZ model A is identified with a product $\Phi_{1,1}\bar{\Phi}_{1,1}$ of chiral primary fields in the left- and right-moving A_2 models, where $\Phi_{1,1}$ ($\bar{\Phi}_{1,1}$) has the conformal dimension $h = 1/6$ and the $U(1)$ charge $q = 1/3$ ($\bar{h} = 1/6$ and $\bar{q} = 1/3$). (The complex conjugate A^* is identified with the product $\Phi_{1,-1}\bar{\Phi}_{1,-1}$, where the anti-chiral primary field $\Phi_{1,-1}$ ($\bar{\Phi}_{1,-1}$) has the same conformal dimension as $\Phi_{1,1}$ ($\bar{\Phi}_{1,1}$) but an opposite $U(1)$ charge.) The central charge of the A_2 model is $c = 1$ (i.e., the Gaussian model). The authors of Ref. [15] obtained finite-size

¹This system is obtained by a dimensional reduction of the four-dimensional Wess-Zumino model [1] from four dimensions to two dimensions.

²A polynomial $W(\Phi)$ of variables Φ_I ($I = 1, 2, \dots, N$) is called quasi-homogeneous when there exist some weights ω_I such that $W(\Phi_I \rightarrow \Lambda^{\omega_I}\Phi_I) = \Lambda W(\Phi)$.

scalings of scalar two-point functions which are remarkably consistent with the above SCFT correspondence, thus demonstrated the power of a lattice formulation of this supersymmetric field theory.³

In this paper, motivated by the success of Ref. [15], we study the 2D $\mathcal{N} = (2, 2)$ WZ model with massless cubic superpotential Eq. (1.1) numerically. We employ a non-perturbative formulation advocated in Ref. [25] that uses a simple momentum cutoff regularization. Although there is an issue concerning the locality in this formulation, the restoration of an expected locality property can be shown at least within perturbation theory [25]. This formulation possesses very nice symmetry properties: it exactly preserves full SUSY, translational invariance, and linear internal symmetries such as the R -symmetry. We believe that these nice symmetry properties are especially useful in defining Noether currents in the regularized framework. In fact, by defining conserved supercurrents and identifying the component of the superconformal currents in the IR limit, we numerically measure the central charge of the system in the IR region: Together with a measurement of the conformal dimension, this forms a main result of the present paper.

Throughout this paper, Greek indices from the middle of the alphabet, μ, ν, \dots run over 0 and 1. Greek indices from the beginning α, β, \dots are for spinor indices and run over 1 and 2. Repeated indices are *not* summed over unless explicit summation symbol is indicated. We extensively use the complex coordinates defined by

$$z \equiv x_0 + ix_1, \quad \bar{z} \equiv x_0 - ix_1, \quad (1.2)$$

and

$$\partial_z \equiv \frac{1}{2}(\partial_0 - i\partial_1), \quad \partial_{\bar{z}} \equiv \frac{1}{2}(\partial_0 + i\partial_1). \quad (1.3)$$

Conjugate momenta are defined by

$$p_z \equiv \frac{1}{2}(p_0 - ip_1), \quad p_{\bar{z}} \equiv \frac{1}{2}(p_0 + ip_1). \quad (1.4)$$

Two-dimensional gamma matrices are defined by

$$\gamma_0 \equiv \begin{pmatrix} 0 & 1 \\ 1 & 0 \end{pmatrix}, \quad \gamma_1 \equiv \begin{pmatrix} 0 & i \\ -i & 0 \end{pmatrix}, \quad (1.5)$$

³For preceding numerical simulations of the 2D $\mathcal{N} = (2, 2)$ WZ model with a *massive* cubic superpotential $W(\Phi) = m\Phi^2/2 + \lambda\Phi^3/3$, see Refs. [17, 18, 19, 20, 21, 22]. See also Refs. [23, 24] for theoretical background.

and

$$\gamma_z \equiv \begin{pmatrix} 0 & 1 \\ 0 & 0 \end{pmatrix}, \quad \gamma_{\bar{z}} \equiv \begin{pmatrix} 0 & 0 \\ 1 & 0 \end{pmatrix}. \quad (1.6)$$

2. Supersymmetric formulation of the 2D $\mathcal{N} = (2, 2)$ WZ model

We start by recapitulating the formulation of Ref. [25]. We suppose that the system is defined in a finite box with a physical size $L_0 \times L_1$. The Fourier modes $\tilde{f}(p)$ of a periodic function in the box are defined by

$$f(x) = \frac{1}{L_0 L_1} \sum_p e^{ipx} \tilde{f}(p), \quad \tilde{f}(p) = \int d^2x e^{-ipx} f(x), \quad (2.1)$$

where the momentum p takes discrete values

$$p_\mu = \frac{2\pi}{L_\mu} n_\mu, \quad n_\mu = 0, \pm 1, \pm 2, \dots, \quad (2.2)$$

and by the definition,

$$\tilde{f}^*(p) = \tilde{f}(-p)^*, \quad (2.3)$$

where the left-hand side denotes the Fourier transformation of the complex conjugate of $f(x)$, $f(x)^*$. In the present formulation [25], we restrict the momentum p by an ultraviolet (UV) cutoff Λ ,

$$-\Lambda \leq p_\mu \leq \Lambda, \quad \text{for } \mu = 0, 1. \quad (2.4)$$

We parametrize this UV cutoff by a “lattice spacing” a ,

$$\Lambda \equiv \frac{\pi}{a}, \quad (2.5)$$

although we do not assume an underlying spacetime lattice structure in this paper (see below). Throughout this paper, all dimensionful quantities are measured in units of the lattice spacing. In particular, if we define the number of lattice points N_μ by

$$L_\mu = N_\mu a, \quad (2.6)$$

then imposing Eq. (2.4) implies

$$-\frac{N_\mu}{2} \leq n_\mu \leq \frac{N_\mu}{2}, \quad \text{for } \mu = 0, 1, \quad (2.7)$$

and thus the number of points in the momentum grid is given by $\sum_p 1 = (N_0 + 1)(N_1 + 1)$.

In the present formulation of the 2D $\mathcal{N} = (2, 2)$ WZ model, the partition function is defined by

$$\mathcal{Z} \equiv \int \prod_{-\Lambda \leq p_\mu \leq \Lambda} \left[d\tilde{A}(p) d\tilde{A}^*(p) \prod_{\alpha=1}^2 d\tilde{\psi}_\alpha(p) \prod_{\dot{\alpha}=\dot{1}}^{\dot{2}} d\tilde{\bar{\psi}}_{\dot{\alpha}}(p) d\tilde{F}(p) d\tilde{F}^*(p) \right] e^{-S}, \quad (2.8)$$

where A , $(\psi_\alpha, \bar{\psi}_{\dot{\alpha}})$, and F are the scalar, fermion and auxiliary fields, respectively. In this expression, the action S is simply the action of the continuum WZ model in terms of Fourier modes:

$$S = \frac{1}{L_0 L_1} \sum_p \left[4p_z \tilde{A}^*(-p) p_{\bar{z}} \tilde{A}(p) - \tilde{F}^*(-p) \tilde{F}(p) - \tilde{F}^*(-p) * W'(\tilde{A})^*(p) - \tilde{F}(-p) * W'(\tilde{A})(p) + (\tilde{\bar{\psi}}_1, \tilde{\bar{\psi}}_2)(-p) \begin{pmatrix} 2ip_z & W''(\tilde{A})^{**} \\ W''(\tilde{A})^* & 2ip_{\bar{z}} \end{pmatrix} \begin{pmatrix} \tilde{\psi}_1 \\ \tilde{\psi}_2 \end{pmatrix}(p) \right], \quad (2.9)$$

where the holomorphic function $W(A)$ is the superpotential and $*$ denotes the convolution

$$(\tilde{\varphi}_1 * \tilde{\varphi}_2)(p) \equiv \frac{1}{L_0 L_1} \sum_q \tilde{\varphi}_1(q) \tilde{\varphi}_2(p - q). \quad (2.10)$$

Products contained in $W'(\tilde{A})$ and $W''(\tilde{A})$ are also understood as convolutions.

Since action (2.9) is identical to that in the continuum theory, the regularized theory (2.8) is manifestly invariant under all symmetries that are consistent with the momentum restriction (2.4). This is the case for symmetry transformations that act linearly on field variables. Thus, in the present formulation, SUSY, translational invariance, and the R -symmetry (if it exists) are exactly preserved. One can derive Ward-Takahashi (WT) identities associated with these symmetries in a regularized framework.

What is sacrificed in the present formulation, on the other hand, is locality. One sees that the kinetic terms and the interaction terms are quite non-local in the configuration space when the UV cutoff Λ is finite. In fact, when both integers N_0 and N_1 are odd, the present formulation is nothing but a two-dimensional version of a lattice formulation of the four-dimensional

WZ model studied in Refs. [26] that is based on the SLAC derivative [27, 28]. A detailed analysis of a one-dimensional version (i.e., quantum mechanics) can be found in Ref. [29]. Thus there is an issue of whether the present formulation reproduces an IR physics expected in the original target theory (i.e., whether it belongs to the same universality class or not). Although one can show [25] that within perturbation theory the expected locality is restored in the limit $\Lambda \rightarrow \infty$ for two- and three-dimensional WZ models, the validity of the present formulation at the non-perturbative level is not obvious *a priori*. We believe that our results in this paper will provide an affirmative indication regarding the question of locality.

As a side remark, we note that the present formulation cannot be regarded as a spacetime lattice formulation when either N_0 or N_1 is even. Fourier modes $\tilde{f}(p)$ of a function $f(x)$ defined on a spacetime lattice is periodic in the Brillouin zone $\tilde{f}(p + (\pi/a)\hat{\mu}) = \tilde{f}(p)$, where $\hat{\mu}$ denotes a unit vector in the μ direction. However, the combination $p_\mu \tilde{f}(p)$ breaks this periodicity at the boundary of the Brillouin zone and thus this cannot be regarded as a Fourier transformation of a function defined on a lattice. (When N_μ are odd, there is no Fourier mode on the boundary of the Brillouin zone.) Throughout this paper we set N_μ even and this means that we lose a connection with a spacetime lattice formulation; we have to regard our configuration space as continuous (with a limited resolution). Still, Eq. (2.8) provides a regularized partition function and can serve as a starting point for non-perturbative study.

3. Simulation algorithm based on the Nicolai map

After integrating over the auxiliary fields \tilde{F} and \tilde{F}^* in Eq. (2.8), the partition function becomes

$$\mathcal{Z} \equiv \int \prod_{-\Lambda \leq p_\mu \leq \Lambda} \left[d\tilde{A}(p) d\tilde{A}^*(p) \prod_{\alpha=1}^2 d\tilde{\psi}_\alpha(p) \prod_{\dot{\alpha}=\dot{1}}^{\dot{2}} d\tilde{\bar{\psi}}_{\dot{\alpha}}(p) \right] e^{-S}, \quad (3.1)$$

where

$$S = \frac{1}{L_0 L_1} \sum_p \left[\tilde{N}^*(-p) \tilde{N}(p) + (\tilde{\psi}_1, \tilde{\psi}_2)(-p) \begin{pmatrix} 2ip_z & W'''(\tilde{A})^{**} \\ W'''(\tilde{A})^* & 2ip_{\bar{z}} \end{pmatrix} \begin{pmatrix} \tilde{\psi}_1 \\ \tilde{\psi}_2 \end{pmatrix}(p) \right]. \quad (3.2)$$

In this expression, $\tilde{N}(p)$ is a function that specifies the Nicolai map [30, 31, 32, 33, 34],

$$\tilde{N}(p) \equiv 2ip_z \tilde{A}(p) + W'(\tilde{A})^*(p), \quad (3.3)$$

$$\tilde{N}^*(-p) = \tilde{N}(p)^* = -2ip_{\bar{z}} \tilde{A}^*(-p) + W'(\tilde{A})(-p). \quad (3.4)$$

For example, for cubic superpotential (1.1), the explicit form of the function $\tilde{N}(p)$ is given by

$$\begin{aligned} \tilde{N}(p) &= i(p_0 - ip_1) \tilde{A}(p) + \lambda \frac{1}{L_0 L_1} \sum_q \tilde{A}^*(q) \tilde{A}^*(p - q) \\ &= i(p_0 - ip_1) \tilde{A}(p) + \lambda \frac{1}{L_0 L_1} \sum_q \tilde{A}(q)^* \tilde{A}(-p - q)^*. \end{aligned} \quad (3.5)$$

We then note

$$S = \frac{1}{L_0 L_1} \sum_p \left[\tilde{N}^*(-p) \tilde{N}(p) + (\tilde{\psi}_1, \tilde{\psi}_2)(-p) \begin{pmatrix} \frac{\partial \tilde{N}(p)}{\partial \tilde{A}(p)} & \frac{\partial \tilde{N}(p)}{\partial \tilde{A}^*(p)} \\ \frac{\partial \tilde{N}^*(p)}{\partial \tilde{A}(p)} & \frac{\partial \tilde{N}^*(p)}{\partial \tilde{A}^*(p)} \end{pmatrix} \begin{pmatrix} \tilde{\psi}_1 \\ \tilde{\psi}_2 \end{pmatrix}(p) \right], \quad (3.6)$$

and therefore, after integrating over fermion fields,

$$\mathcal{Z} \equiv \int \prod_{-\Lambda \leq p_\mu \leq \Lambda} [d\tilde{A}(p) d\tilde{A}^*(p)] \exp \left[\frac{1}{L_0 L_1} \sum_p \tilde{N}^*(-p) \tilde{N}(p) \right] \det \frac{\partial(\tilde{N}, \tilde{N}^*)}{\partial(\tilde{A}, \tilde{A}^*)}. \quad (3.7)$$

In this partition function, we may change integration variables from $(\tilde{A}(p), \tilde{A}^*(p))$ to $(\tilde{N}(p), \tilde{N}^*(p))$. Then the Jacobian associated with this change of variables precisely cancels the absolute value of the fermion determinant. In this way, we arrive at the expression

$$\begin{aligned} \mathcal{Z} &= \int \prod_{-\Lambda \leq p_\mu \leq \Lambda} [d\tilde{N}(p) d\tilde{N}^*(p)] \exp \left[-\frac{1}{L_0 L_1} \sum_p \tilde{N}(p)^* \tilde{N}(p) \right] \\ &\quad \times \sum_i \text{sign} \det \frac{\partial(\tilde{N}, \tilde{N}^*)}{\partial(\tilde{A}, \tilde{A}^*)} \bigg|_{\tilde{A}=\tilde{A}_i, \tilde{A}^*=\tilde{A}_i^*}, \end{aligned} \quad (3.8)$$

where $\tilde{A}(p)_i$ and $\tilde{A}^*(p)_i$ ($i = 1, 2, \dots$) are solutions of

$$2ip_z \tilde{A}(p) + W'(\tilde{A})(-p)^* - \tilde{N}(p) = 0, \quad (3.9)$$

$$-2ip_{\bar{z}} \tilde{A}(p)^* + W'(\tilde{A})(-p) - \tilde{N}(p)^* = 0. \quad (3.10)$$

Representation (3.8) for the partition function (and a similar representation for expectation values of observables) gives rise to the following simulation algorithm [17, 15]: (i) Generate Gaussian random numbers $(\tilde{N}(p), \tilde{N}(p)^*)$. (ii) Find (numerically) all the solutions $(\tilde{A}(p)_i, \tilde{A}(p)_i^*)$ ($i = 1, 2, \dots$) of Eqs. (3.9) and (3.10). (iii) Then compute the sums

$$\sum_i \text{sign det} \frac{\partial(\tilde{N}, \tilde{N}^*)}{\partial(\tilde{A}, \tilde{A}^*)} \Big|_{\tilde{A}=\tilde{A}_i, \tilde{A}^*=\tilde{A}_i^*}, \quad (3.11)$$

and

$$\sum_i \text{sign det} \frac{\partial(\tilde{N}, \tilde{N}^*)}{\partial(\tilde{A}, \tilde{A}^*)} \mathcal{O}(\tilde{A}, \tilde{A}^*) \Big|_{\tilde{A}=\tilde{A}_i, \tilde{A}^*=\tilde{A}_i^*}, \quad (3.12)$$

where $\mathcal{O}(\tilde{A}, \tilde{A}^*)$ is an observable. (iv) Repeat the steps from (i) and take an average over the Gaussian random numbers. The expectation value of an observable \mathcal{O} is given by

$$\langle \mathcal{O} \rangle = \frac{1}{\Delta} \frac{\left\langle \sum_i \text{sign det} \frac{\partial(\tilde{N}, \tilde{N}^*)}{\partial(\tilde{A}, \tilde{A}^*)} \mathcal{O}(\tilde{A}, \tilde{A}^*) \Big|_{\tilde{A}=\tilde{A}_i, \tilde{A}^*=\tilde{A}_i^*} \right\rangle_N}{\langle 1 \rangle_N}, \quad (3.13)$$

where $\langle \cdot \rangle_N$ denotes the average over the Gaussian random numbers and

$$\Delta \equiv \frac{\left\langle \sum_i \text{sign det} \frac{\partial(\tilde{N}, \tilde{N}^*)}{\partial(\tilde{A}, \tilde{A}^*)} \Big|_{\tilde{A}=\tilde{A}_i, \tilde{A}^*=\tilde{A}_i^*} \right\rangle_N}{\langle 1 \rangle_N}. \quad (3.14)$$

As Eq. (3.13) shows, in the present algorithm the expectation value of an observable $\langle \mathcal{O} \rangle$ is given by the ratio of two expectation values with respect to the Gaussian random numbers. In this paper, we apply a simple propagation of error rule to the ratio to estimate the statistical error in $\langle \mathcal{O} \rangle$. This procedure must be good enough because the statistical error in the denominator of the ratio, Δ , is generally quite small (see below).

Since the above simulation algorithm is based on the generation of the Gaussian random numbers, there is no autocorrelation among generated configurations and there is no critical slowing down; this is an overwhelming advantage of the present simulation algorithm.⁴ Another interesting feature of

⁴We would like thank Martin Lüscher for bringing our attention to this point.

this algorithm is that the “normalized partition function” Δ in Eq. (3.14) can be argued to give the Witten index $\text{tr}(-1)^F$ [35].⁵ For the massive free theory $W(\Phi) = m\Phi^2/2$, one easily sees that $\Delta = 1$ and reproduces the correct Witten index $\text{tr}(-1)^F = 1$. Thus assuming that the proportionality constant between the partition function defined by the functional integral and $\text{tr}(-1)^F$ is independent of the interaction, we have $\Delta = \text{tr}(-1)^F$. It is known that for a homogeneous superpotential $W(\Phi) = \lambda\Phi^n/n$, $\text{tr}(-1)^F = n - 1$. Therefore, the relation $\Delta = n - 1$ provides a quantitative test of the simulation [15].

A disadvantage of the present simulation algorithm is that it is not *a priori* clear how many solutions $(\tilde{A}(p)_i, \tilde{A}(p)_i^*)$ that Eqs. (3.9) and (3.10) have. Thus we cannot be completely sure whether we have found all the solutions or not. Another limitation of the algorithm is that it is applicable only to supersymmetric boundary conditions; so it cannot explore physics with the finite temperature, for example.

4. Simulation parameters

In this paper, we fix the coupling constant in Eq. (1.1) to be

$$a\lambda = 0.3. \quad (4.1)$$

This is the same choice of the coupling constant as Ref. [15], provided that our parameter a in Eq. (2.5) is identified with the lattice spacing in Ref. [15]. The size of the momentum grid $N_0 \times N_1$ is varied from 16×16 to 36×36 . For each value of $N_0 \times N_1$, we generated 1280 configurations of the Gaussian random numbers $(\tilde{N}(p), \tilde{N}(p)^*)$. We then solved Eqs. (3.9) and (3.10) by using the Newton-Raphson (NR) method [37]. The solution $(\tilde{A}(p), \tilde{A}(p)^*)$ depends on the initial guess in the NR method and, as the initial guess, we used 100 random configurations $(\tilde{A}(p), \tilde{A}(p)^*)$ generated with Gaussian random numbers with a unit variant. We judged that the convergence of the NR method is achieved when the maximum norm of the residue of Eqs. (3.9) and (3.10) becomes smaller than 10^{-13} . Two obtained solutions were regarded identical when the the maximum norm of the difference of the solutions is smaller than 10^{-11} . In this way, we obtained configurations tabulated in Tables 1 and 2. The total amount of computational time was 34307.7 core · hour on the Intel Xeon 2.93GHz. In Tables 1 and 2, configurations are classified

⁵With conventional simulation algorithms, one needs more elaborate method to compute the Witten index; see Ref. [36].

Table 1: Classification of obtained configurations. Δ is given by Eq. (3.14) and δ is defined by Eq. (5.8).

$N_0 = N_1$	16	18	20	22	24	26
(+, +)	1276	1273	1275	1271	1271	1273
(-, +, +, +)	4	7	5	9	9	7
(+)	0	0	0	0	0	0
(+, +, +)	0	0	0	0	0	0
(-, +, +, +, +)	0	0	0	0	0	0
(-, -, +, +, +, +)	0	0	0	0	0	0
Δ	2	2	2	2	2	2
δ [%]	0.2(2)	0.1(1)	-0.2(1)	0.1(1)	-0.1(1)	-0.1(1)

Table 2: Classification of obtained configurations (cont'd). Δ is given by Eq. (3.14) and δ is defined by Eq. (5.8).

$N_0 = N_1$	28	30	32	34	36
(+, +)	1264	1261	1250	1254	1221
(-, +, +, +)	16	17	24	17	26
(+)	0	1	2	6	31
(+, +, +)	0	0	4	2	2
(-, +, +, +, +)	0	1	0	0	0
(-, -, +, +, +, +)	0	0	0	1	0
Δ	2	2.000(1)	2.002(2)	1.997(2)	1.977(4)
δ [%]	-0.0(1)	0.1(2)	0.0(2)	-0.1(3)	0.0(5)

according to the number of associated solutions $(\tilde{A}(p)_i, \tilde{A}(p)_i^*)$ and the associated sign of the Jacobian [15]. For example, an entry in a row with the symbol $(-, +, +, +)$ implies that there was a configuration of $(\tilde{N}(p), \tilde{N}(p)^*)$ for which we have four different solutions $(\tilde{A}(p)_i, \tilde{A}(p)_i^*)$ ($i = 1, 2, 3, 4$) and the sign of the Jacobian is negative for one of them and it is positive for other three. Thus, we can read off Δ in Eq. (3.14) from this table. We see that the expected relation $\Delta = 2$ for cubic superpotential (1.1) actually holds almost within one percent even for the worst case, for $N_0 \times N_1 = 36 \times 36$. This fact suggests that even if our root-finding code missed some of solutions of Eqs. (3.9) and (3.10), they are precious few.

5. SUSY WT identities

WT identities associated with exact symmetries in the formulation provide a consistency check for the numerical simulation. In particular, since SUSY is an exact symmetry in the present formulation, SUSY WT identities must hold even with a *finite* UV cutoff. This aspect is quite different from conventional lattice formulations in which one hopes that SUSY is restored only in the continuum limit. Thus an explicit confirmation of SUSY WT identities in the present formulation is interesting in its own right.

SUSY transformations in the 2D $\mathcal{N} = (2, 2)$ WZ model are given by Q_1 , Q_2 , Q_1 , and Q_2 . In terms of Fourier modes, they are given by

$$\begin{aligned}
Q_1 \tilde{\psi}_1(p) &= -2\sqrt{2}ip_z \tilde{A}^*(p), & Q_1 \tilde{A}^*(p) &= 0, \\
Q_1 \tilde{F}^*(p) &= 2\sqrt{2}ip_z \tilde{\psi}_2(p), & Q_1 \tilde{\psi}_2(p) &= 0, \\
Q_1 \tilde{A}(p) &= \sqrt{2}\tilde{\psi}_1(p), & Q_1 \tilde{\psi}_1(p) &= 0, \\
Q_1 \tilde{\psi}_2(p) &= \sqrt{2}\tilde{F}(p), & Q_1 \tilde{F}(p) &= 0,
\end{aligned} \tag{5.1}$$

for Q_1 ,

$$\begin{aligned}
Q_2 \tilde{\psi}_2(p) &= -2\sqrt{2}ip_z \tilde{A}^*(p), & Q_2 \tilde{A}^*(p) &= 0, \\
Q_2 \tilde{F}^*(p) &= -2\sqrt{2}ip_z \tilde{\psi}_1(p), & Q_2 \tilde{\psi}_1(p) &= 0, \\
Q_2 \tilde{A}(p) &= \sqrt{2}\tilde{\psi}_2(p), & Q_2 \tilde{\psi}_2(p) &= 0, \\
Q_2 \tilde{\psi}_1(p) &= -\sqrt{2}\tilde{F}(p), & Q_2 \tilde{F}(p) &= 0,
\end{aligned} \tag{5.2}$$

for Q_2

$$\begin{aligned}
\bar{Q}_1 \tilde{\psi}_1(p) &= -2\sqrt{2}ip_z \tilde{A}(p), & \bar{Q}_1 \tilde{A}(p) &= 0, \\
\bar{Q}_1 \tilde{F}(p) &= -2\sqrt{2}ip_z \tilde{\psi}_2(p), & \bar{Q}_1 \tilde{\psi}_2(p) &= 0, \\
\bar{Q}_1 \tilde{A}^*(p) &= \sqrt{2} \tilde{\psi}_1(p), & \bar{Q}_1 \tilde{\psi}_1(p) &= 0, \\
\bar{Q}_1 \tilde{\psi}_2(p) &= -\sqrt{2} \tilde{F}^*(p), & \bar{Q}_1 \tilde{F}^*(p) &= 0,
\end{aligned} \tag{5.3}$$

for \bar{Q}_1 ,

$$\begin{aligned}
\bar{Q}_2 \tilde{\psi}_2(p) &= -2\sqrt{2}ip_z \tilde{A}(p), & \bar{Q}_2 \tilde{A}(p) &= 0, \\
\bar{Q}_2 \tilde{F}(p) &= 2\sqrt{2}ip_z \tilde{\psi}_1(p), & \bar{Q}_2 \tilde{\psi}_1(p) &= 0, \\
\bar{Q}_2 \tilde{A}^*(p) &= \sqrt{2} \tilde{\psi}_2(p), & \bar{Q}_2 \tilde{\psi}_2(p) &= 0, \\
\bar{Q}_2 \tilde{\psi}_1(p) &= \sqrt{2} \tilde{F}^*(p), & \bar{Q}_2 \tilde{F}^*(p) &= 0,
\end{aligned} \tag{5.4}$$

for \bar{Q}_2 .

A simple one-point SUSY WT identity is given by [18]

$$0 = \langle S \rangle = \langle S_B \rangle + \left(\sum_p 1 - 2 \sum_p 1 \right) = \langle S_B \rangle - (N_0 + 1)(N_1 + 1), \tag{5.5}$$

where S_B is the bosonic part of the action after integrating over the auxiliary field, giving by

$$S_B \equiv \frac{1}{L_0 L_1} \sum_p \tilde{N}^*(-p) \tilde{N}(p). \tag{5.6}$$

In Eq. (5.5), the first equality holds because the action S in Eq. (2.9) can be written as

$$\begin{aligned}
S = -\frac{1}{2}Q \frac{1}{L_0 L_1} \sum_p \Big\{ & \left[2ip_z \tilde{A}^*(-p) + \tilde{F}^*(-p) + 2W'(\tilde{A})^* \right] \tilde{\psi}_1(p) \\
& + \left[-2ip_z \tilde{A}(p) + \tilde{F}(p) + 2W'(\tilde{A})^* \right] \tilde{\psi}_2(-p) \Big\}, \tag{5.7}
\end{aligned}$$

where $Q \equiv -(\bar{Q}_1 + Q_2)/\sqrt{2}$ is a nilpotent SUSY transformation. Therefore $\langle S \rangle = 0$ provided SUSY is not spontaneously broken, as the non-zero Witten index in the present system shows. One can then exactly evaluate the expectation value of the parts of the action which are quadratic in the auxiliary

field and the fermion field; this gives the second equality in Eq. (5.5). Since $\sum_p 1 = (N_0 + 1)(N_1 + 1)$, we have the last equality in Eq. (5.5). That is, we have

$$\delta \equiv \frac{\langle S_B \rangle}{(N_0 + 1)(N_1 + 1)} - 1 = 0. \quad (5.8)$$

This relation provides a quantitative test of the simulation [18, 15].⁶ We show δ in Tables 1 and 2 for each value of $N_0 \times N_1$ and see that relation (5.8) holds within 0.5%.

As for a two-point SUSY WT identity, from the relation $\langle Q_1(\tilde{A}(p)\tilde{\psi}_1(-p)) \rangle = 0$, we consider

$$p_0 \langle \tilde{A}(p)\tilde{A}^*(-p) \rangle = -\text{Im} \langle \tilde{\psi}_1(p)\tilde{\psi}_1(-p) \rangle. \quad (5.9)$$

In Fig. 1, we plotted both sides of this relation for our coarsest grid ($N_0 \times N_1 = 16 \times 16$) as a function of ap_0 ; both sides coincide within the statistical error.

For more quantitative comparison, we plotted in Fig. 2 the ratio of the left-hand side and the right-hand side again as a function of ap_0 . (The error in the ratio was estimated by a simple propagation of error rule.) We plotted the cases of $N_0 \times N_1 = 16 \times 16$ and $N_0 \times N_1 = 36 \times 36$. For both cases of the momentum grid, the identity holds within $\sim 5\%$, a good indication of SUSY.

Similarly, from $\langle Q_2(\tilde{F}^*(p)\tilde{\psi}_1(-p)) \rangle = 0$, we have⁷

$$\langle \tilde{F}(p)\tilde{F}^*(-p) \rangle = -p_1 \text{Re} \langle \tilde{\psi}_1(p)\tilde{\psi}_1(-p) \rangle + p_0 \text{Im} \langle \tilde{\psi}_1(p)\tilde{\psi}_1(-p) \rangle. \quad (5.11)$$

The results for this identity are depicted in Figs. 3 and 4.⁸

⁶Lattice formulations adopted in Refs. [18] and [15] and more generally lattice formulations based on the Nicolai map [23, 17, 18, 16, 24, 19, 20, 21] possess exact invariance under the above nilpotent Q transformation. See also Ref. [38] and references therein.

⁷In the Wess-Zumino model, the integration over the auxiliary field is defined by an analytic continuation, and according to this prescription, the correlation function is expressed as

$$\langle \tilde{F}(p)\tilde{F}^*(-p) \rangle = \left\langle \left[-\tilde{N}(p) + 2ip_z\tilde{A}(p) \right] \left[-\tilde{N}^*(-p) - 2ip_z\tilde{A}^*(-p) \right] \right\rangle - L_0L_1, \quad (5.10)$$

in terms of a correlation function of the Gaussian random fields and the scalar fields. The last term gives a negative contribution, and despite its appearance, the left-hand side can be negative as our plot shows.

⁸Since $\langle \tilde{F}(0)\tilde{F}^*(0) \rangle = -\langle Q_2(\tilde{\psi}_1(0)\tilde{F}^*(0)) \rangle / \sqrt{2}$, $\langle \tilde{F}(p)\tilde{F}^*(-p) \rangle$ evaluated at $p = 0$ must vanish if SUSY is not spontaneously broken. Our plot in Fig. 3 is consistent with this expectation.

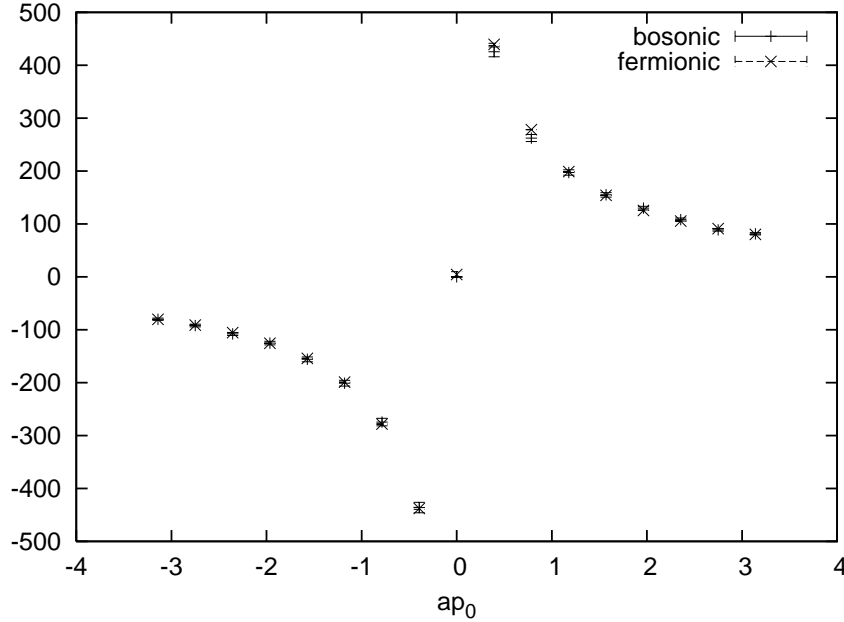


Figure 1: The left-hand side (“bosonic”) and the right-hand side (“fermionic”) of Eq. (5.9) as a function of ap_0 along the line $ap_1 = 0$; $N_0 \times N_1 = 16 \times 16$.

Having obtained these encouraging results concerning SUSY in our numerical simulation, let us proceed to study physical questions.

6. Conformal dimension of a chiral primary field

As noted in the Introduction, in the IR limit, the scalar field A in the WZ model with cubic potential (1.1) is expected to behave as a product $\Phi_{1,1} \bar{\Phi}_{1,1}$ of chiral primary fields in the left- and right-moving A_2 models, where $\Phi_{1,1}$ and $\bar{\Phi}_{1,1}$ have the conformal dimensions $h = 1/6$ and $\bar{h} = 1/6$, respectively. For such a field with conformal dimensions (h, \bar{h}) , the two-point function will behave as

$$\langle A(x) A^*(0) \rangle \propto \frac{1}{z^{2h} \bar{z}^{2\bar{h}}}, \quad \text{for } |x| \text{ large.} \quad (6.1)$$

Then assuming that A is spinless, $h = \bar{h}$, the anomalous dimension $h + \bar{h} = 2h$ could be extracted from the susceptibility of the scalar field χ_ϕ , defined by [15]

$$\chi_\phi \equiv \frac{1}{a^2} \int_{L_0 L_1} d^2 x \langle A(x) A^*(0) \rangle = \frac{1}{a^2 L_0 L_1} \left\langle \left| \tilde{A}(0) \right|^2 \right\rangle, \quad (6.2)$$

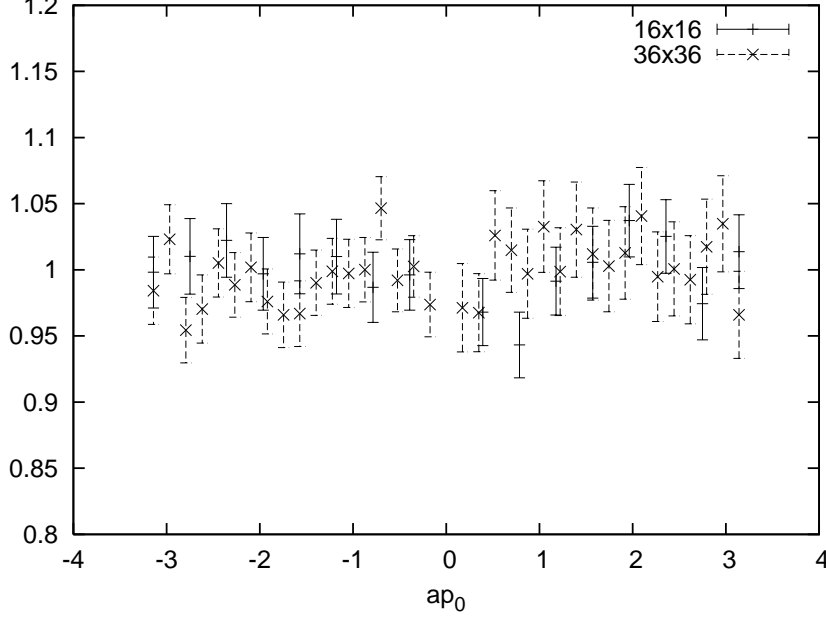


Figure 2: The ratio of the left-hand side and the right-hand side of Eq. (5.9) as a function of ap_0 along the line $ap_1 = 0$ (the origin $p = 0$ is excluded from the plot). The cases of $N_0 \times N_1 = 16 \times 16$ and $N_0 \times N_1 = 36 \times 36$ are plotted.

as

$$\chi_\phi \propto \int_{L_0 L_1} d^2 x \frac{1}{(x^2)^{2h}} \propto (L_0 L_1)^{1-h-\bar{h}}, \quad \text{for } L_\mu \text{ large.} \quad (6.3)$$

Thus $\ln(\chi_\phi)$ would be a linear function of $\ln(L_0 L_1)$ for large L_μ and $1 - h - \bar{h}$ is obtained by the slope of the linear function [15]. In Fig. 5, we plot $\ln(\chi_\phi)$ as a function of $\ln(a^{-2} L_0 L_1)$ (recall that in our present simulation the lattice spacing is fixed to $a\lambda = 0.3$). From the plot, we see that a fit by a linear function would be good for large sizes as $a^{-2} L_0 L_1 \gtrsim 24 \times 24$. Therefore, we applied a linear χ^2 fit by using data from $N_0 \times N_1 = 24 \times 24$ to $N_0 \times N_1 = 36 \times 36$. To estimate a systematic error associated with this choice of fitting range, we also carried out a linear fit using data from $N_0 \times N_1 = 26 \times 26$ to $N_0 \times N_1 = 36 \times 36$. See Table 3

In Eq. (6.2), the integral over x is performed for all x including the coincidence point $x = 0$. This might be physically unnatural because the coincidence point $x = 0$ would suffer from ambiguity associated with the UV regularization. On the other hand, true long-distance physics should be

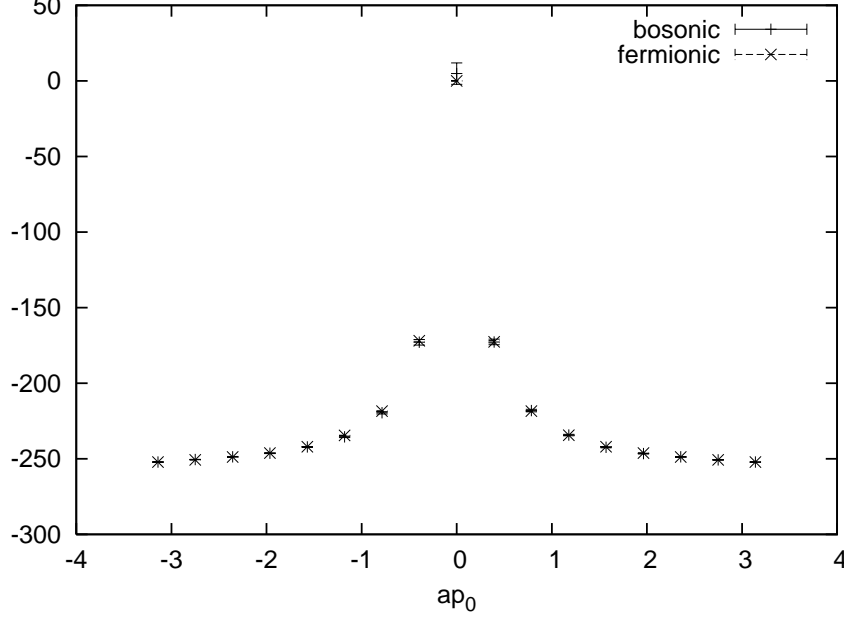


Figure 3: The left-hand side (“bosonic”) and the right-hand side (“fermionic”) of Eq. (5.11) along the line $ap_1 = 0$; $N_0 \times N_1 = 16 \times 16$.

independent of such a UV ambiguity. To avoid such UV ambiguity and to estimate how much our determination depends on the UV prescription, we could define the susceptibility with the UV part subtracted [15]:

$$\begin{aligned}
\chi_\phi &\equiv \frac{1}{a^2} \int_{L_0 L_1 - n_0 n_1 a^2} d^2 x \langle A(x) A^*(0) \rangle \\
&= \frac{1}{a^2 L_0 L_1} \left\langle \left| \tilde{A}(0) \right|^2 \right\rangle \\
&\quad - \frac{1}{a^2 (L_0 L_1)^2} \sum_p \frac{2}{p_0} \sin \left(\frac{p_0 a n_0}{2} \right) \frac{2}{p_1} \sin \left(\frac{p_1 a n_1}{2} \right) \left\langle \left| \tilde{A}(p) \right|^2 \right\rangle, \quad (6.4)
\end{aligned}$$

where the integral has been defined by extracting a region $a^2 n_0 \times n_1$ containing the coincidence point $x = 0$; in this expression it is understood that $(2/p_\mu) \sin(p_\mu a n_\mu/2) = a n_\mu$ for $p_\mu = 0$. Figure 6 is the result with the UV subtraction with $n_0 \times n_1 = 3 \times 3$ (this is a choice identical to Ref. [15]). Our linear fits are summarized in Table 3. By adopting the average of the second and the third rows in Table 3 as the central value and estimating a

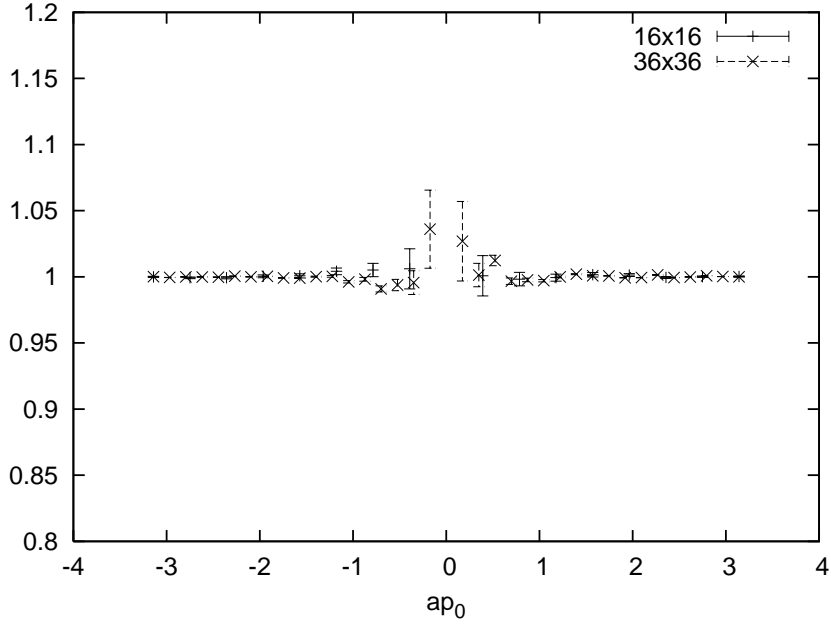


Figure 4: The ratio of the left-hand side and the right-hand side of Eq. (5.11) as a function of ap_0 along the line $ap_1 = 0$ (the origin $p = 0$ is excluded from the plot). The cases of $N_0 \times N_1 = 16 \times 16$ and $N_0 \times N_1 = 36 \times 36$ are plotted.

systematic error associated with the fitting range and the UV ambiguity by variations in Table 3, we quote

$$1 - h - \bar{h} = 0.616(25)(13). \quad (6.5)$$

This value is somewhat smaller than the value obtained in Ref. [15], but still consistent with the expected exact value $1 - h - \bar{h} = 2/3 = 0.666\dots$ within 1.3σ .

7. Central charge from a supercurrent correlator

The central charge c , defined by the Virasoro anomaly

$$\langle T_{zz}(x)T_{zz}(0) \rangle = \frac{1}{8\pi^2} \frac{c/2}{z^4}, \quad (7.1)$$

where T_{zz} is the holomorphic part of the energy-momentum tensor, is a fundamental quantity that characterizes a conformal field theory (CFT). It is

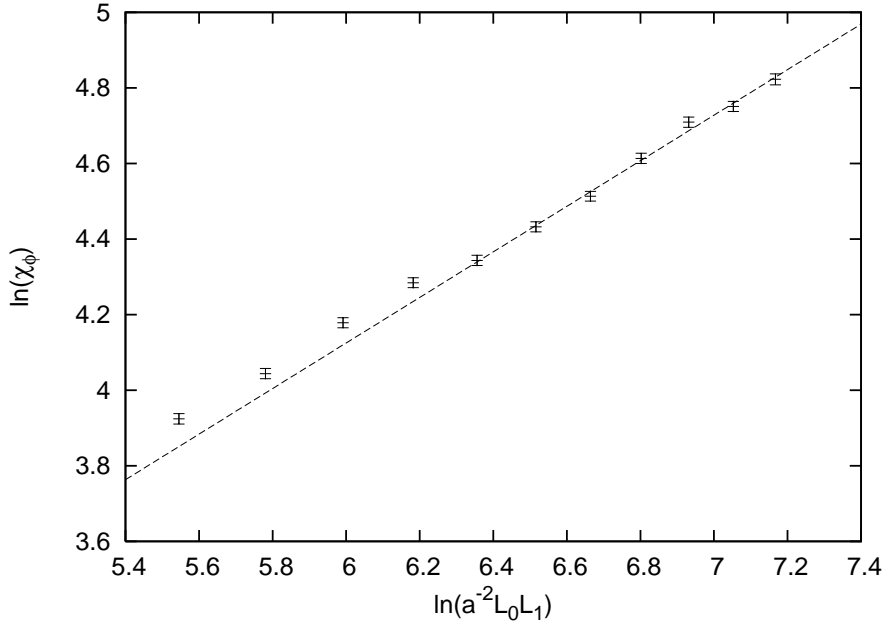


Figure 5: $\ln(\chi_\phi)$ as a function of $\ln(a^{-2}L_0L_1)$. No UV subtraction is made. The broken line is a linear fit with $1 - h - \bar{h} = 0.603$.

thus of great interest whether we can measure this quantity c in the IR region from the present numerical simulation and obtain further support for the conjectured correspondence between the WZ model and SCFT. A salient feature of the present formulation is its nice symmetry properties, including translational invariance. Thus, we may define the energy-momentum tensor as a Noether current associated with the translational invariance in a regularized framework.

In an $\mathcal{N} = 2$ SCFT, the central charge c appears also in the correlation function between the holomorphic $U(1)$ currents:

$$\langle J_z(x) J_z(0) \rangle = \frac{1}{8\pi^2} \frac{c/3}{z^2}. \quad (7.2)$$

In the LG description, the $U(1)$ symmetry in the $\mathcal{N} = 2$ SCFT is identified with the $U(1)_R$ symmetry of the WZ model with a (quasi-)homogeneous superpotential (see below) and this $U(1)_R$ is also exactly preserved in the present formulation. We can thus define a conserved $U(1)_R$ current whose appropriate component is identified with J_z .

Table 3: Linear χ^2 fit used for a determination of the anomalous dimension in Eq. (6.5). $n_0 \times n_1$ denotes the UV subtraction region defined in Eq. (6.4).

$n_0 \times n_1$	fitting range of $N_0 \times N_1$	$\chi^2/\text{d.o.f.}$	$1 - h - h$
0×0	from 24×24 to 36×36	0.904	0.603(19)
0×0	from 26×26 to 36×36	1.088	0.609(25)
3×3	from 24×24 to 36×36	0.910	0.624(20)
3×3	from 26×26 to 36×36	1.108	0.629(26)

In preliminary numerical study of the above two-point functions of *bosonic* operators (T_{zz} for Eq. (7.1) and J_z for Eq. (7.2)), however, we found that signals are generally very noisy and reliable fits for the central charge would be rather difficult.⁹ So, in what follows, we adopt a different approach that employs a two-point function of the $\mathcal{N} = 2$ superconformal currents:

$$\langle G_z^+(x) G_z^-(0) \rangle = \frac{1}{8\pi^2} \frac{2c/3}{z^3}. \quad (7.3)$$

Since the operators G_z^\pm are *fermionic*, there is no “disconnected diagram” which could contribute to Eq. (7.3) and we expect a clear signal from numerical simulation. In fact the following results seem to be in accord with this naive expectation.

Now, since our present formulation possesses exact SUSY, we can define a conserved supercurrent. To obtain this, we consider the localized SUSY transformation (for a generic field φ)

$$\delta\tilde{\varphi}(p) = \frac{1}{L_0 L_1} \sum_q \left[\sum_{\alpha=1}^2 \tilde{\xi}^\alpha(q) Q_\alpha \tilde{\varphi}(p-q) - \sum_{\dot{\alpha}=1}^2 \tilde{\xi}^{\dot{\alpha}}(q) \bar{Q}_{\dot{\alpha}} \tilde{\varphi}(p-q) \right], \quad (7.4)$$

where $\tilde{\xi}^\alpha(q)$ and $\tilde{\xi}^{\dot{\alpha}}(q)$ are non-constant Grassmann parameters and Q_α and $\bar{Q}_{\dot{\alpha}}$ are defined by Eqs. (5.1)–(5.4). Then from the variation of the

⁹We stress that this preliminary study was quite incomplete. In particular, we have not seriously considered the necessity of subtracting some disconnected parts from correlation functions. Clearly additional study is needed to conclude something about the use of those correlation functions in computation of the central charge.

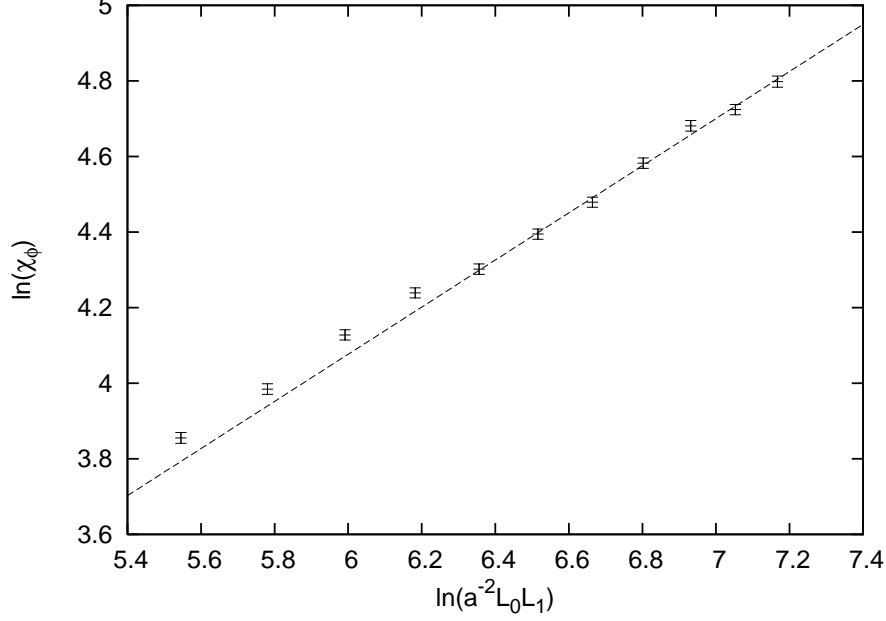


Figure 6: $\ln(\chi_\phi)$ as a function of $\ln(a^{-2}L_0L_1)$. UV subtraction Eq. (6.4) with $n_0 \times n_1 = 3 \times 3$ is made. The broken line is a linear fit with $1 - h - \bar{h} = 0.624$.

action, we define supercurrents $\tilde{S}_\mu^\pm(p)$ and $\tilde{\tilde{S}}_\mu^\pm(p)$ as

$$\begin{aligned} \delta S \equiv \frac{1}{L_0L_1} \sum_p (-2) \sum_\mu & \left[\tilde{\xi}^2(-p)(-ip_\mu)\tilde{S}_\mu^+(p) + \tilde{\xi}^2(-p)(-ip_\mu)\tilde{S}_\mu^-(p) \right. \\ & \left. + \tilde{\xi}^1(-p)(-ip_\mu)\tilde{\tilde{S}}_\mu^+(p) + \tilde{\xi}^1(-p)(-ip_\mu)\tilde{\tilde{S}}_\mu^-(p) \right]. \end{aligned} \quad (7.5)$$

By construction, above supercurrents satisfy SUSY WT identities, such as

$$p_\mu \left\langle \tilde{S}_\mu^+(p) \tilde{\varphi}_1(q_1) \dots \tilde{\varphi}_n(q_n) \right\rangle = \frac{i}{2} \sum_{i=1}^n \left\langle \tilde{\varphi}_1(q_1) \dots \bar{Q}_2 \tilde{\varphi}_i(q_i + p) \dots \tilde{\varphi}_n(q_n) \right\rangle. \quad (7.6)$$

This identity would imply that (according to the standard argument) the current \tilde{S}_μ^+ is a correctly normalized operator.

In Eq. (7.5), the explicit form of the supercurrents are given by

$$\tilde{S}_z^+(p) = \frac{1}{L_0 L_1} \sum_q \sqrt{2} i (p - q)_z \tilde{A}(p - q) \tilde{\psi}_2(q), \quad (7.7)$$

$$\tilde{S}_{\bar{z}}^+(p) = \frac{1}{L_0 L_1} \sum_q \frac{1}{\sqrt{2}} W'(\tilde{A})(p - q) \tilde{\psi}_1(q), \quad (7.8)$$

$$\tilde{S}_z^-(p) = -\frac{1}{L_0 L_1} \sum_q \sqrt{2} i (p - q)_z \tilde{A}^*(p - q) \tilde{\psi}_2(q), \quad (7.9)$$

$$\tilde{S}_{\bar{z}}^-(p) = \frac{1}{L_0 L_1} \sum_q \frac{1}{\sqrt{2}} W'(\tilde{A})^*(p - q) \tilde{\psi}_1(q), \quad (7.10)$$

and

$$\tilde{\tilde{S}}_z^+(p) = \frac{1}{L_0 L_1} \sum_q \sqrt{2} i (p - q)_z \tilde{A}(p - q) \tilde{\psi}_1(q), \quad (7.11)$$

$$\tilde{\tilde{S}}_z^-(p) = -\frac{1}{L_0 L_1} \sum_q \frac{1}{\sqrt{2}} W'(\tilde{A})(p - q) \tilde{\psi}_2(q), \quad (7.12)$$

$$\tilde{\tilde{S}}_{\bar{z}}^-(p) = -\frac{1}{L_0 L_1} \sum_q \sqrt{2} i (p - q)_{\bar{z}} \tilde{A}^*(p - q) \tilde{\psi}_1(q), \quad (7.13)$$

$$\tilde{\tilde{S}}_z^-(p) = -\frac{1}{L_0 L_1} \sum_q \frac{1}{\sqrt{2}} W'(\tilde{A})^*(p - q) \tilde{\psi}_2(q). \quad (7.14)$$

A Noether current is, however, always ambiguous as one can change the definition as $\tilde{S}_z^\pm(p) \rightarrow \tilde{S}_z^\pm(p) + p_z \tilde{X}^\pm(p)$ and $\tilde{S}_{\bar{z}}^\pm(p) \rightarrow \tilde{S}_{\bar{z}}^\pm(p) - p_{\bar{z}} \tilde{X}^\pm(p)$ by using certain combinations $\tilde{X}^\pm(p)$ without affecting the conservation law, $p_{\bar{z}} \tilde{S}_z^\pm(p) + p_z \tilde{S}_{\bar{z}}^\pm(p) = 0$. To fix this ambiguity, we required in Eqs. (7.7) to (7.14) that

$$\tilde{S}_z^+ = \tilde{S}_{\bar{z}}^- = \tilde{\tilde{S}}_z^+ = \tilde{\tilde{S}}_{\bar{z}}^- = 0, \quad (7.15)$$

when $W' = 0$. The WZ model with $W' = 0$ is a massless free theory that itself is an $\mathcal{N} = (2, 2)$ SCFT. For this system it is natural to adopt a supercurrent that obeys the gamma-traceless condition,

$$\sum_\mu \gamma_\mu \begin{pmatrix} \tilde{\tilde{S}}_\mu^- \\ \tilde{\tilde{S}}_\mu^+ \end{pmatrix} = \sum_\mu \gamma_\mu \begin{pmatrix} \tilde{\tilde{S}}_\mu^+ \\ \tilde{\tilde{S}}_\mu^- \end{pmatrix} = 0, \quad (7.16)$$

because this condition is a super-partner of the traceless condition $T_{z\bar{z}} = 0$ [39] that is usually assumed in CFT. Eq. (7.15) is nothing but Eq. (7.16) in components.

Thus we had a natural definition of the supercurrents. We then postulate a correspondence between the components of above supercurrents and the holomorphic part of the superconformal currents in the IR limit. That is,

$$\tilde{S}_z^+(p) \rightarrow \tilde{G}_z^+(p), \quad \tilde{S}_z^-(p) \rightarrow \tilde{G}_z^-(p). \quad (7.17)$$

Our reasoning for this correspondence is as follow: (i) The conservation law of the supercurrents in the coordinate space yields $\partial_{\bar{z}} S_z^\pm(x) + \partial_z S_{\bar{z}}^\pm(x) = 0$. In the IR limit, the derivative of the superpotential $W'(A)$ is expected to become irrelevant (see, for example, §14.4 of Ref. [12]) so $S_{\bar{z}}^\pm(x)$, from explicit forms (7.8) and (7.10), could be neglected in the IR limit. Then the conservation law implies that $S_z^\pm(x)$ are holomorphic functions, a correct property of $G_z^\pm(x)$. (ii) The WZ model with a homogeneous superpotential $W = \lambda \Phi^n/n$ possesses the $U(1)_R$ symmetry

$$\begin{aligned} A &\rightarrow e^{(2/n)i\theta} A, & \psi_\alpha &\rightarrow e^{-(1-2/n)i\theta} \psi_\alpha, \\ \bar{\psi}_{\dot{\alpha}} &\rightarrow e^{(1-2/n)i\theta} \bar{\psi}_{\dot{\alpha}}, & F &\rightarrow e^{-(2-2/n)i\theta} F, \end{aligned} \quad (7.18)$$

which is, in the IR, identified with a $U(1)$ symmetry generated by a *sum* of two $U(1)$ currents J_z and $\bar{J}_{\bar{z}}$, where J_z and $\bar{J}_{\bar{z}}$ are $U(1)$ currents in the left- and right-moving $\mathcal{N} = 2$ superconformal algebras, respectively (see, for example, §19.4 of Ref. [11]). Thus, in Eq. (7.18), the $U(1)_R$ charge of the scalar field A is assigned $2/n$, because A is identified with a product $\Phi_{1,1} \bar{\Phi}_{1,1}$ of chiral primary fields in the left- and right-moving A_{n-1} models, in which $\Phi_{1,1}$ has the $U(1)$ charge $q = 1/n$ and $\bar{\Phi}_{1,1}$ has the $U(1)$ charge $\bar{q} = 1/n$. Then, according to the $U(1)$ charge assignment in Eq. (7.18), we see that \tilde{S}_z^+ in Eq. (7.7) possesses the $U(1)$ charge $+1$, a correct $U(1)$ charge of G_z^+ with respect to J_z . Similarly, \tilde{S}_z^- in Eq. (7.9) possesses the $U(1)$ charge -1 , a correct $U(1)$ charge of G_z^- with respect to J_z . (iii) The overall normalization of the supercurrents has been fixed such that Eq. (7.3) is reproduced under correspondence (7.17) for the massless free theory ($W' = 0$). This theory itself is an $\mathcal{N} = (2, 2)$ SCFT whose left-moving sector possesses the central charge $c = 3$ (one complex scalar and two Majorana-Weyl fermions).

Thus, under identification (7.17), our procedure is as follows: we numerically compute the two-point function of the supercurrents in the momentum

space

$$\left\langle \tilde{S}_z^+(p) \tilde{S}_z^-(-p) \right\rangle. \quad (7.19)$$

Then, in view of correspondence (7.17), we compare this function in the IR region¹⁰ $|p| \lesssim \lambda$ with the two-point function of the superconformal currents in the momentum space

$$\begin{aligned} L_0 L_1 \int d^2x e^{-ipx} \langle G_z^+(x) G_z^-(0) \rangle &= L_0 L_1 \frac{-ic}{48\pi} \frac{\partial^3}{\partial p_z^3} \frac{p^2}{\delta^2} K_2(|p|\delta) \\ &\xrightarrow{|p|\delta \rightarrow 0} L_0 L_1 \frac{ic}{24\pi} \frac{p_z^2}{p_{\bar{z}}}, \end{aligned} \quad (7.20)$$

where we have used Eq. (7.3) that is, strictly speaking, an expression valid only on \mathbb{R}^2 . In deriving the last expression, we regularized the singularity in the integrand at $x = 0$ by setting $1/z^3 = (\bar{z})^3/(x^2)^3 \rightarrow (\bar{z})^3/(x^2 + \delta^2)^3$; note that the last low-momentum behavior (i.e., the IR physics) in Eq. (7.20) is independent of the regularization parameter δ .

For the above computation, we used only data with the finest grid $N_0 \times N_1 = 36 \times 36$. In Fig. 7, we depicted the real part of correlation function (7.19) as a function of ap_0 along the line $ap_1 = \pi/18 \sim 0.1745$. The broken line is the real part of function (7.20) with $c = 1$; it agrees well with the data for $|ap_0| \leq \pi/18 \sim 0.1745 < 0.3$, a good indication for $c \sim 1$ in the IR region. Fig. 8 is the same as Fig. 7, but for the imaginary part. The broken line is the imaginary part of function (7.20) with $c = 1$; this time it agrees well with the data for $|ap_0| \leq 2\pi/18 \sim 0.349 \simeq 0.3$.

Our fit for c proceeds as follows: We first consider the real part of the ratio of correlation function (7.19) to the function $L_0 L_1 (i/24\pi) p_z^2/p_{\bar{z}}$ appearing in Eq. (7.20). For illustration, the real part of this ratio along several constant ap_1 lines are depicted in Figs. 9, 10 and 11. We see that actually the ratio is close to 1 around the origin in the momentum space $|p| \sim 0$. Then, to use data points with a fixed energy scale, we define a fitting region $R(b_1, b_2)$ on the momentum grid as illustrated in Fig. 12. Then we carry out a χ^2 fit by a constant for data points in the fitting region $R(b_1, b_2)$. Since the IR region is characterized by the condition $|ap| \lesssim a\lambda = 0.3$ and the lowest non-zero momentum in the present $N_0 \times N_1 = 36 \times 36$ momentum grid is

¹⁰Note that the coupling constant λ in Eq. (1.1) is a unique physical dimensional parameter in the present system.

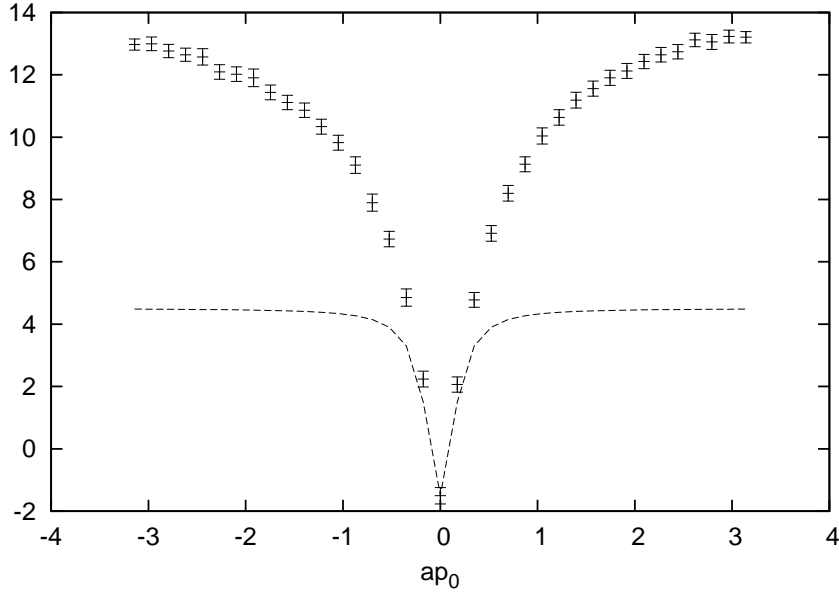


Figure 7: The real part of the correlation function (7.19) as a function of ap_0 along the line $ap_1 = \pi/18 \sim 0.1745$; $N_0 \times N_1 = 36 \times 36$. The broken line is the real part of function (7.20) with $c = 1$.

$ap_\mu = \pi/18 \sim 0.1745$, we regard the fitting region $R(1, 1)$, or at most $R(1, 2)$, as the IR region; see Table 4. From the numbers in the table, we estimate

$$c = 1.09(14)(31), \quad (7.21)$$

as the central charge in the IR region. Our estimate reproduces the conjectured value $c = 1$ very well.

Although strictly speaking expression (7.20) is meaningful only for very small momenta and the LG description is expected to be valid only for the

Table 4: Results of a χ^2 fit used for a determination of the central charge c in (7.21).

fitting region	number of data points	$\chi^2/\text{d.o.f.}$	c
$R(1, 1)$	8	1.93	1.09(14)
$R(1, 2)$	24	3.50	1.40(8)

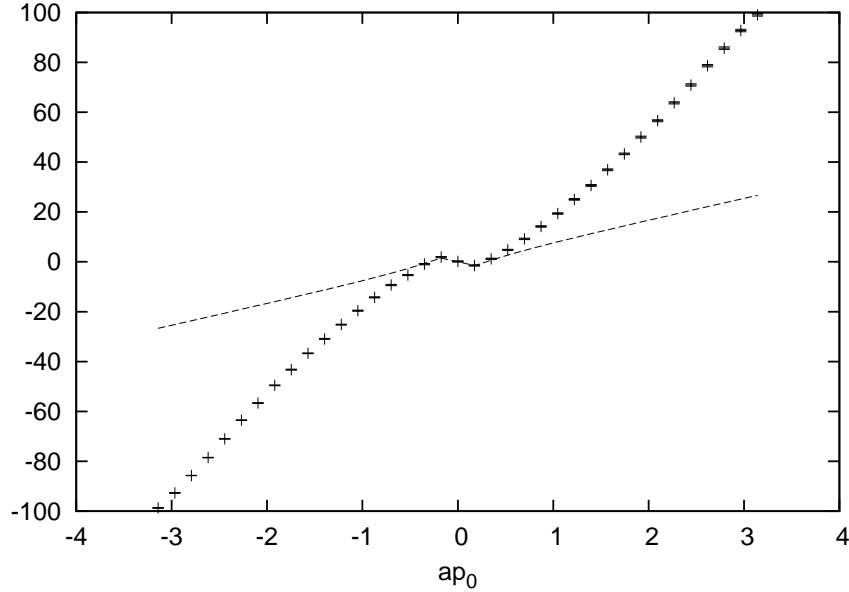


Figure 8: The imaginary part of the correlation function (7.19) as a function of ap_0 along the line $ap_1 = \pi/18 \sim 0.1745$; $N_0 \times N_1 = 36 \times 36$. The broken line is the imaginary part of function (7.20) with $c = 1$.

low-energy region $|ap| \lesssim a\lambda = 0.3$, we found that it is nevertheless interesting to repeat the above procedure for “intermediate” energy $|ap| \gtrsim a\lambda = 0.3$ or even “high” energy $|ap| \sim \pi$ regions. Figures 13 and 14 is a result of the fitting in an “intermediate” energy region $|ap| \sim 0.7$. We observe a rather good fit with an “effective c ”, $c \sim 2$. We may repeat such a fit by changing the parameter b in $R(b, b)$ which roughly corresponds to the energy scale. The result of such fits as a function of b are shown in Fig. 15. It is interesting that, going from the UV side to the IR side, the plot goes from $c \sim 3$, the central charge corresponding to the massless free theory, and decreases to $c \sim 1$, the central charge of the A_2 model. Although one should not take this plot so seriously because χ^2 becomes quite large for large b (for example, $\chi^2/\text{d.o.f.} \sim 19$ for $b = 8$), it is still interesting to note an analogue of the Zamolodchikov C function [40] in this plot; the C function monotonically decreases along the renormalization group flow from UV to IR and coincides with the central charge at a fixed point. It is an interesting problem to clarify the underlying reason for this similarity of Fig. 15 with the C function.

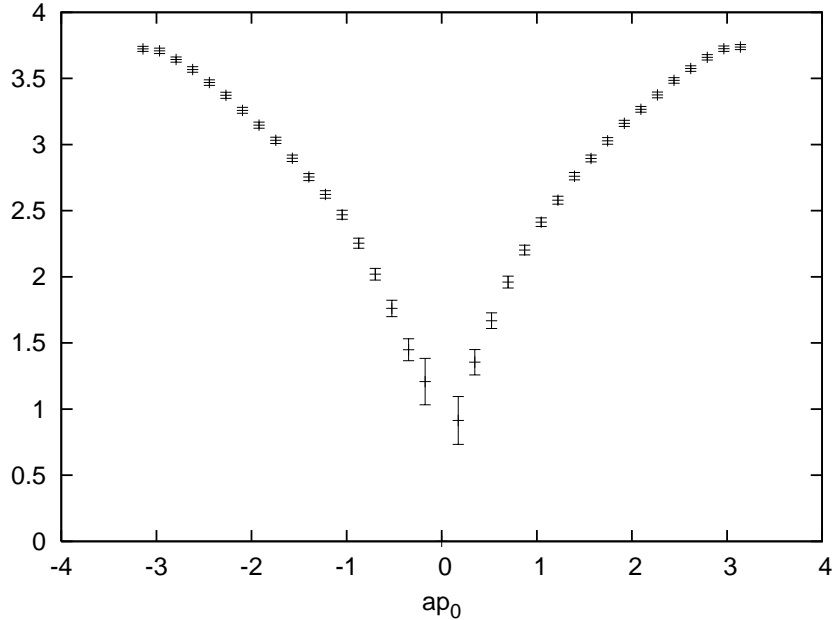


Figure 9: The real part of the ratio of the correlation function (7.19) and the function $L_0 L_1(i/24\pi)p_z^2/p_{\bar{z}}$ as a function of ap_0 along the line $ap_1 = 0$; $N_0 \times N_1 = 36 \times 36$. The origin $p = 0$ is excluded from the plot because $p_z^2/p_{\bar{z}}$ is singular at the origin.

8. Conclusion

In this paper, we carried out a non-perturbative numerical study of low-energy physics of the 2D WZ model with the massless cubic superpotential. We obtained the critical exponent $1 - h - \bar{h}$ and the central charge c which are consistent with the conjectured emergence of a non-trivial $\mathcal{N} = (2, 2)$ SCFT, thus provided further support for the LG description. Our results indicate that our supersymmetric non-perturbative formulation of the WZ model is working, although there has been an issue concerning the locality in this formulation. For further improvement of these results, better observables which yield less systematic errors should be investigated. Also, we want to generalize the present analysis to higher critical LG models.

We would like to thank Michael G. Endres, Kazuo Fujikawa, Masafumi Fukuma, Daisuke Kadoh, Hikaru Kawai, Akitsugu Miwa, and Tsuneo Uematsu for discussions and comments. We are quite indebted to Hiroki Kawai and Yoshio Kikukawa for discussions and detailed explanation on the simulation in Ref. [15] and to Michael G. Endres for a careful reading of the

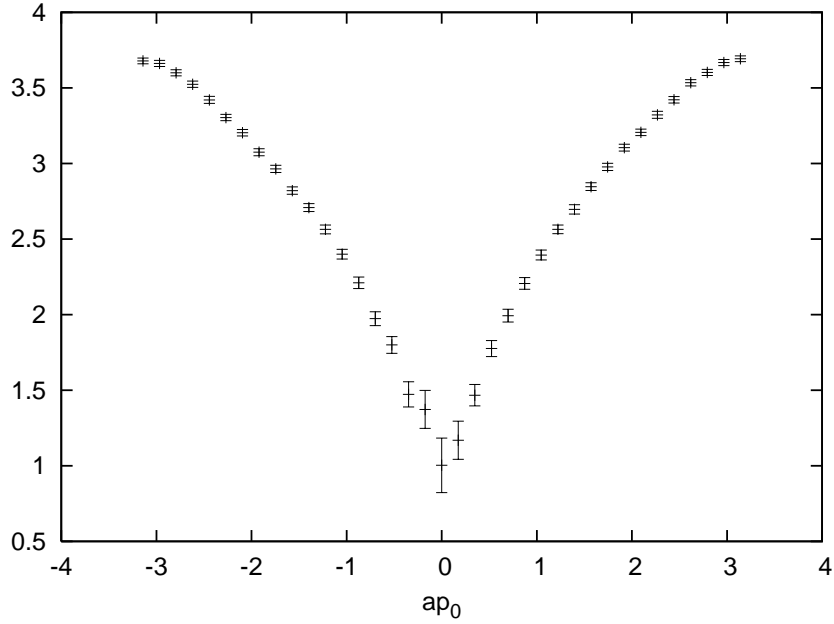


Figure 10: The real part of the ratio of the correlation function (7.19) and the function $L_0 L_1 (i/24\pi) p_z^2 / p_{\bar{z}}$ as a function of ap_0 along the line $ap_1 = \pi/18 \sim 0.1745$; $N_0 \times N_1 = 36 \times 36$.

manuscript. Our numerical calculations were carried out by using the RIKEN Integrated Cluster of Clusters (RICC) facility. The work of H.S. is supported in part by a Grant-in-Aid for Scientific Research, 22340069 and 23540330.

References

- [1] J. Wess and B. Zumino, Nucl. Phys. B **70** (1974) 39.
- [2] D. A. Kastor, E. J. Martinec and S. H. Shenker, Nucl. Phys. B **316** (1989) 590.
- [3] C. Vafa and N. P. Warner, Phys. Lett. B **218** (1989) 51.
- [4] W. Lerche, C. Vafa and N. P. Warner, Nucl. Phys. B **324** (1989) 427.
- [5] P. S. Howe and P. C. West, Phys. Lett. B **223** (1989) 377.
- [6] S. Cecotti, L. Girardello and A. Pasquinucci, Nucl. Phys. B **328** (1989) 701.

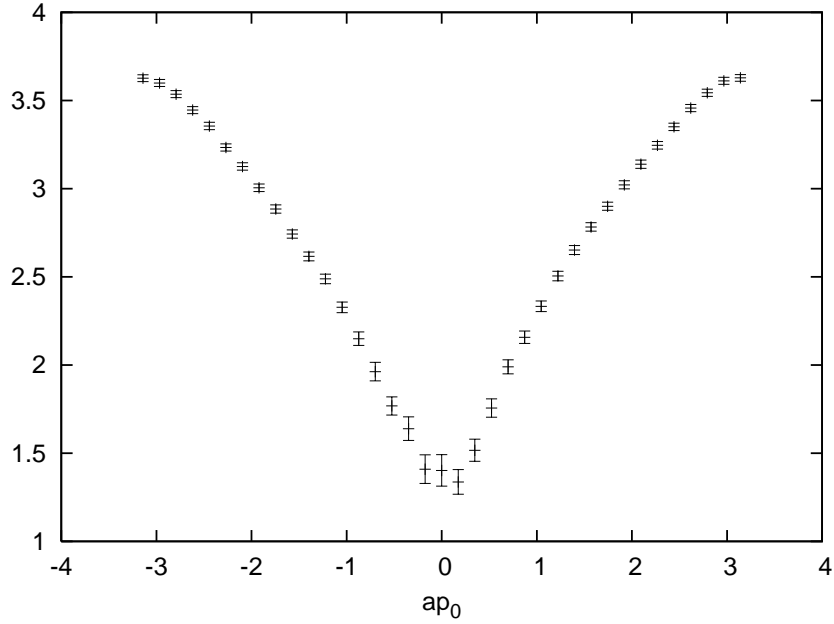


Figure 11: The real part of the ratio of the correlation function (7.19) and the function $L_0 L_1(i/24\pi)p_z^2/p_{\bar{z}}$ as a function of ap_0 along the line $ap_1 = 2\pi/18 \sim 0.349$; $N_0 \times N_1 = 36 \times 36$.

- [7] P. S. Howe and P. C. West, Phys. Lett. B **227** (1989) 397.
- [8] S. Cecotti, L. Girardello and A. Pasquinucci, Int. J. Mod. Phys. A **6** (1991) 2427.
- [9] S. Cecotti, Int. J. Mod. Phys. A **6** (1991) 1749.
- [10] E. Witten, Int. J. Mod. Phys. A **9** (1994) 4783 [arXiv:hep-th/9304026].
- [11] J. Polchinski, “String theory. Vol. 2: Superstring theory and beyond,” *Cambridge, UK: Univ. Pr. (1998) 531 p*
- [12] K. Hori *et al.*, “Mirror symmetry,” *Providence, USA: AMS (2003) 929 p*
- [13] A. B. Zamolodchikov, Sov. J. Nucl. Phys. **44** (1986) 529 [Yad. Fiz. **44** (1986) 821].
- [14] E. Witten, Nucl. Phys. B **403** (1993) 159 [arXiv:hep-th/9301042].

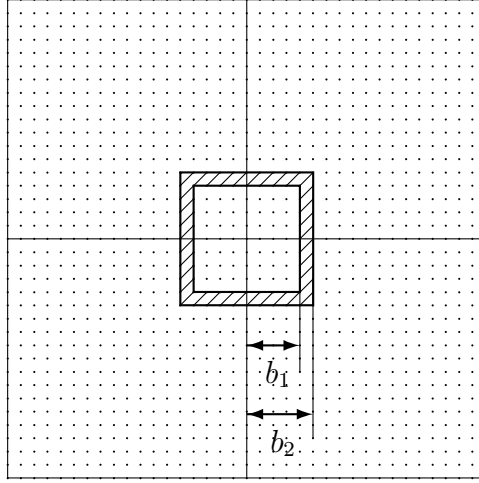


Figure 12: The fitting region $R(b_1, b_2)$ on the $N_0 \times N_1 = 36 \times 36$ momentum grid. Data points at the boundaries as well as data points inside the shaded region are used for a constant fit.

- [15] H. Kawai and Y. Kikukawa, Phys. Rev. D **83** (2011) 074502 [arXiv:1005.4671 [hep-lat]].
- [16] Y. Kikukawa and Y. Nakayama, Phys. Rev. D **66** (2002) 094508 [arXiv:hep-lat/0207013].
- [17] M. Beccaria, G. Curci and E. D'Ambrosio, Phys. Rev. D **58** (1998) 065009 [arXiv:hep-lat/9804010].
- [18] S. Catterall and S. Karamov, Phys. Rev. D **65** (2002) 094501 [arXiv:hep-lat/0108024].
- [19] J. Giedt, Nucl. Phys. B **726** (2005) 210 [arXiv:hep-lat/0507016].
- [20] G. Bergner, T. Kaestner, S. Uhlmann and A. Wipf, Annals Phys. **323** (2008) 946 [arXiv:0705.2212 [hep-lat]].
- [21] T. Kästner, G. Bergner, S. Uhlmann, A. Wipf and C. Wozar, Phys. Rev. D **78** (2008) 095001 [arXiv:0807.1905 [hep-lat]].
- [22] F. Synatschke-Czerwonka, T. Fischbacher and G. Bergner, Phys. Rev. D **82** (2010) 085003 [arXiv:1006.1823 [hep-th]].
- [23] N. Sakai and M. Sakamoto, Nucl. Phys. B **229** (1983) 173.

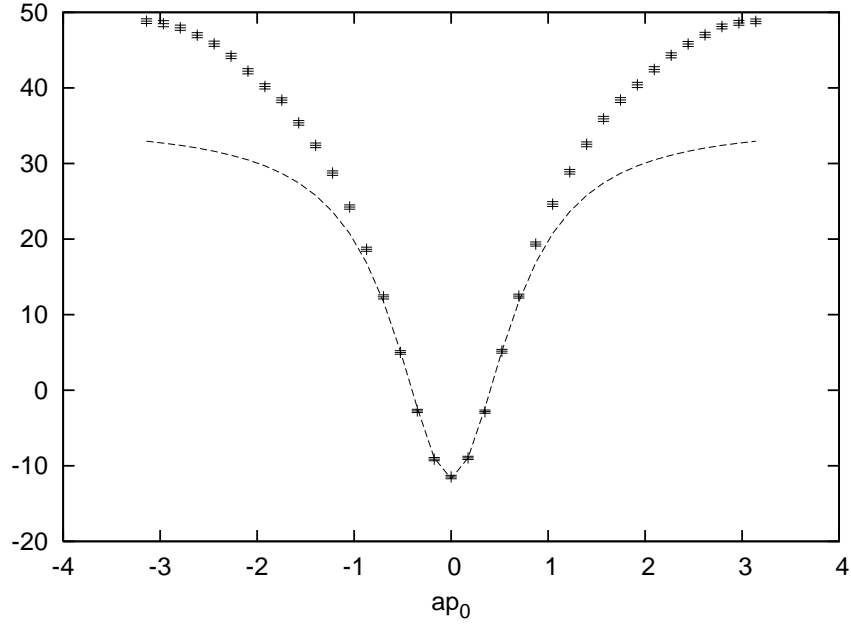


Figure 13: The real part of the correlation function (7.19) as a function of ap_0 along the line $ap_1 = 4\pi/18 \sim 0.698$; $N_0 \times N_1 = 36 \times 36$. The broken line is the real part of function (7.20) with $c = 1.95$, that was obtained by a constant fit in the fitting region $R(4, 4)$ ($\chi^2/\text{d.o.f.} = 1.58$).

- [24] K. Fujikawa, Phys. Rev. D **66** (2002) 074510 [arXiv:hep-lat/0208015].
- [25] D. Kadoh and H. Suzuki, Phys. Lett. B **684** (2010) 167 [arXiv:0909.3686 [hep-th]].
- [26] J. Bartels and J. B. Bronzan, Phys. Rev. D **28** (1983) 818.
- [27] S. D. Drell, M. Weinstein and S. Yankielowicz, Phys. Rev. D **14** (1976) 487.
- [28] S. D. Drell, M. Weinstein and S. Yankielowicz, Phys. Rev. D **14** (1976) 1627.
- [29] G. Bergner, JHEP **1001** (2010) 024 [arXiv:0909.4791 [hep-lat]].
- [30] H. Nicolai, Phys. Lett. B **89** (1980) 341.
- [31] H. Nicolai, Nucl. Phys. B **176** (1980) 419.

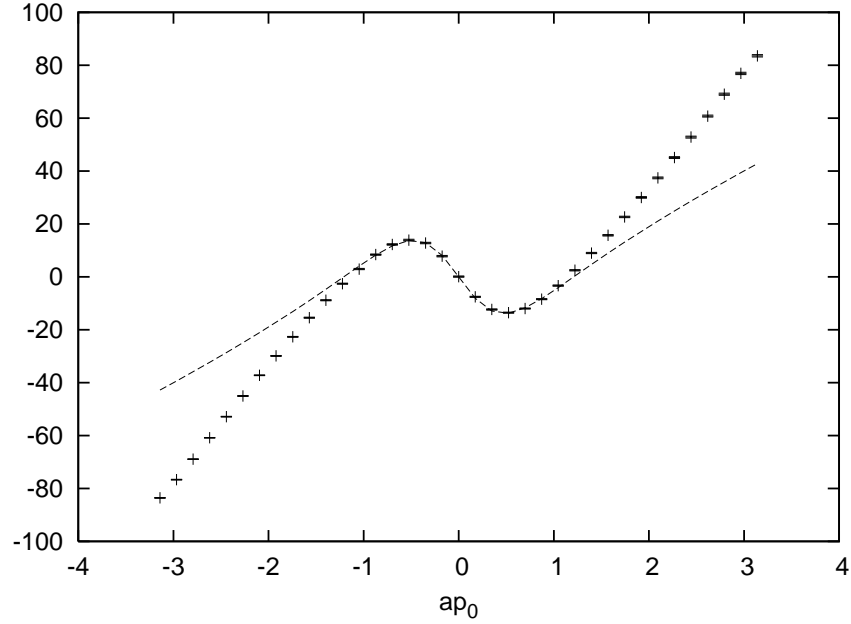


Figure 14: The imaginary part of the correlation function (7.19) as a function of ap_0 along the line $ap_1 = 4\pi/18 \sim 0.698$; $N_0 \times N_1 = 36 \times 36$. The broken line is the imaginary part of function (7.20) with $c = 1.95$.

- [32] S. Cecotti and L. Girardello, Phys. Lett. B **110** (1982) 39.
- [33] G. Parisi and N. Surlas, Nucl. Phys. B **206** (1982) 321.
- [34] S. Cecotti and L. Girardello, Nucl. Phys. B **226** (1983) 417.
- [35] E. Witten, Nucl. Phys. B **202** (1982) 253.
- [36] I. Kanamori, Nucl. Phys. B **841** (2010) 426 [arXiv:1006.2468 [hep-lat]].
- [37] W. H. Press, S. A. Teukolsky, W. T. Vetterling and B. P. Flannery, “Numerical Recipes. The Art of Scientific Computing, 3rd Edition,” *New York, USA: Cambridge University Press (2007) 1235 p*
- [38] D. Kadoh and H. Suzuki, Phys. Lett. B **696** (2011) 163 [arXiv:1011.0788 [hep-lat]].
- [39] S. Ferrara and B. Zumino, Nucl. Phys. B **87** (1975) 207.

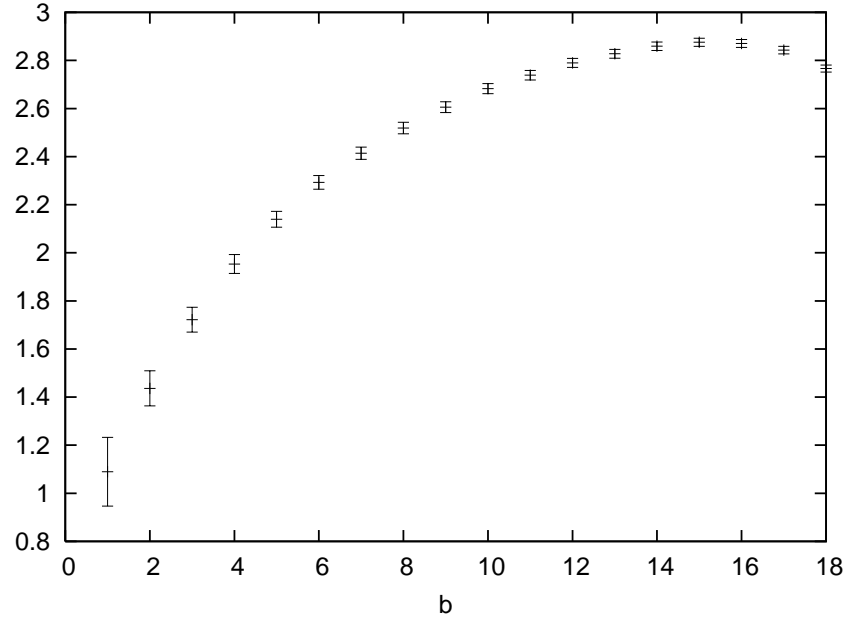


Figure 15: “Effective c ” obtained from a constant fit in the fitting region $R(b, b)$.

- [40] A. B. Zamolodchikov, JETP Lett. **43** (1986) 730 [Pisma Zh. Eksp. Teor. Fiz. **43** (1986) 565].